Central European Journal of Energetic Materials
ISSN 1733-7178; e-ISSN 2353-1843

Cent. Eur. J. Energ. Mater. 2017, *14*(3): 589-604; DOI: 10.22211/cejem/76241

Studies on the Effect of Nano-MnO_2 in HTPB-based Composite Propellant Formulations

Dhirendra R. Kshirsagar, Sunil Jain, Sumit Bhandarkar, Manoj Vemuri, Mehilal*

High Energy Materials Research Laboratory,
Sutarwadi, Pune-411021, India
**E-mail: drmehilal@yahoo.co.in*

Abstract: Various propellant compositions were prepared incorporating fully characterized nano-sized manganese dioxide, from 0.25 wt.% to 1.0 wt.%, in HTPB/AP/Al-based composite propellant formulations having 86 wt.% of solid loading, and its effects on the viscosity build-up, thermal, mechanical and ballistic properties were studied. The findings revealed that on increasing the percentage of nano-MnO_2 in the composition, there was an increase in the end of mix viscosity, the modulus and tensile strength, while the elongation decreased accordingly. The data on the thermal properties revealed a reduction in the decomposition temperature of ammonium perchlorate (AP) as well as of the formulations based on it. The data on the ballistic properties revealed that there is an enhancement in the burning rate from 6.11 mm/s (reference composition) to 7.54 mm/s at 6.86 MPa (a 23% enhancement in the burning rate) and an increase in the pressure exponent from 0.35 (reference composition) to 0.42 with 1.0 wt.% nano-MnO_2.

Keywords: composite propellant, nano-manganese dioxide, pressure exponent, burning rate

1 Introduction

Composite solid propellants are composed of an elastomeric polymeric binder, in which solid particles of oxidizer, fuel, and additives are incorporated. It basically contains an oxidizer such as ammonium perchlorate (AP), or potassium perchlorate (KP), or ammonium dinitramide (ADN), *etc*. [1, 2]; a binder such as cured hydroxyl terminated polybutadiene (HTPB) and a metallic fuel such as

aluminium powder, along with certain process aids and ballistic modifiers [3]. The burning rate of composite propellants is considered to be one of the most important properties governing the ballistic performance of solid rocket motors, which in turn depends mostly on the particle characteristics of the oxidizers, burning rate catalysts and metallic fuel [4]. To achieve the desired burning rate of composite propellant formulations, the amount of oxidizer, the particle sizes of the oxidizer and burning rate modifiers are used as variables. AP is used as an oxidizer in composite propellant formulations as the major ingredient [5], in different size fractions to enhance its density and also its burning rate. Fine and superfine particle fractions of AP increase the burning rate, but the viscosity of the propellant slurry is also increased, thus creating slurry casting difficulties [6]. Therefore, to cope with such problems, burning rate modifiers are preferred. The burning rate modifiers commonly used in composite propellant formulations are transition metal oxides (TMOs) or transition metal complexes [7]. Burning rate modifiers affect the burning rate by lowering the thermal decomposition temperature of AP. The effect of transition metal oxides on the thermal decomposition of AP has been studied and reviewed by various workers [7, 8]. Many researchers have studied in detail the effect of micron-sized TMOs, such as Fe_2O_3, CuO, MnO_2, Co_2O_3, NiO and Cr_2O_3, on the ballistic properties, mainly the burning rate behaviour of composite propellants and found substantial increases in the burning rate [9, 10]. Another approach to enhance the burning rate of composite propellant formulations is the incorporation of transition metal complexes and transition metal complexes grafted on to binders such as ferrocene, catocene and butacene [11, 12].

The burning rate of propellant formulations is greatly affected by the use of catalysts of smaller particle size. Smaller particles create larger interfacial areas and increase the number of atoms or molecules at the particle interface, which in turn enhances the catalytic activity. Recently many researchers have reported the application of nano-sized catalysts for the enhancement of the burning rate of composite propellants [13-15].

Manganese oxohydroxide (MnOOH) nanocrystals [16] dispersed on graphene and nano Mn_3O_4-graphene (Mn_3O_4-GR) hybrids [17] were studied with AP as well as AP-based composite propellants and found to be effective in reducing the thermal decomposition temperature of AP by 80 °C and 141.9 °C, respectively. The effect of nano-$MnFe_2O_4$ particles [18], prepared by the co-precipitation method and the combustion method, on the thermal decomposition of AP was also studied and revealed that ferrite type mixed oxides reduce the thermal decomposition temperature by 77.3 °C and 84.9 °C, respectively. Furthermore, Chandru *et al.* [19] evaluated the effect of the mesoporous β-MnO_2 on the thermal

decomposition of AP and as a ballistic modifier in AP-based compositions. The results revealed that the mesoporous β-MnO_2 is very effective in catalysing decomposition of AP (reducing the decomposition temperature by 153 °C with 2 wt.% catalyst). Naya *et al.* [20] studied ammonium nitrate(V) (AN)-HTPB-based composites supplemented with MnO_2 as a burning catalyst and found that MnO_2 improves the burning characteristics of AN-based propellants. In other work, mixed oxides of copper, chromium, manganese, *etc*. have been used in different ratios to study the burning behaviour of AP/HTPB propellants and it was found that catalysts containing copper oxide mixtures have a reinforcing capability compared to mixtures containing no copper oxide, resulting in higher burning rates [21]. Kohga *et al*. investigated the thermal decomposition behaviour and burning characteristics of AN/RDX based composite propellants supplemented with MnO_2 and Fe_2O_3 and their results revealed that mixed catalysts were more promising than individual catalysts in enhancing the burning rate [22]. Kishore *et al*. reported the catalytic effect of Fe_2O_3, Ni_2O_3, MnO_2 and Co_2O_3 on AP/CTPB and AP/PS propellant systems and found that Ni_2O_3 and Fe_2O_3 were more effective than MnO_2 in enhancing the burning rate [23]. Also, Singh *et al.* studied the catalytic activity of nano-MnO_2 crystals on the thermal decomposition of AP and found that it enhances the thermal decomposition [24].

A systematic study of the mix viscosity, mechanical, thermal and ballistic properties of composite propellant formulations (86 wt.%) on incorporating nano-MnO_2 has been carried out. The results reported here are compared with a reference composition, as well as with micron-sized MnO_2.

2 Experimental

2.1 Materials

Both nano- and micron-sized manganese dioxide, AR grade, were purchased from Nanoshel (USA). AP, procured from M/s Pandian Chemicals Ltd. (Cuddalore, India), was used in a bimodal distribution having average particle sizes 300 μm and 50 μm in the ratio of 3.5:1, respectively. HTPB, manufactured by free radical solution polymerization and having an average molecular weight ($\overline{M}_n$) of 2560 with a hydroxyl number of 43 mg KOH/g, was procured from M/s Anabond Ltd. (Chennai, India). Aluminium powder, having average particle size 15 ± 3 μm, was procured from M/s The Metal Powder Company (Madurai, India) and was used as received. Dioctyl adipate (DOA), toluene di-isocyanate (TDI), N-phenyl-2-naphthylamine (NONOX-D), trimethylolpropane (TMP) and 1,4-butanediol (n-BD) were also procured from trade and used as received.

2.2 Characterization

The material and phase identification of nano/micron-sized MnO_2 was determined with a Phillips PANalytical X'Pert[3] Powder X-ray diffractometer using Cu K_α radiation in the range 20° to 90°. The purity of nano-MnO_2 was determined by Inductively Coupled Plasma-Atomic Emission Spectroscopy (ICP-AES) Model: JY Ultima 2000, France. The particle size of nano-MnO_2 was determined with a NANOPHOX particle size analyzer (NX0084), Germany, based on the dynamic light scattering technique in aqueous medium after sonication for 5 min. The particle size of micron-MnO_2 was determined by laser based particle size analyser CILAS, model 1064L, France, in aqueous medium. The particle size and surface morphology of nano/micron-sized MnO_2 was also determined by Field Emission Scanning Electron Microscopy (FESEM) FEI Nova NanoSEM 450 with a resolution capability of 1.4 nm. The specific surface area (SSA) of nano-MnO_2/micron-MnO_2 was determined with a BET surface area analyser, Gemini VII 2390 t, Micromeritics, USA, based on the nitrogen adsorption technique after degassing the sample at 250 °C for 6 h followed by the determination of the surface area at liquid nitrogen temperature (77 K).

A Brookfield dial type viscometer, Model HBT, was used for the measurement of the end of mix (EOM) viscosity of the propellant slurry by a T-C spindle at a rotation speed of 2.5 rpm at 40 °C. Thermal studies on the decomposition were carried out on a differential scanning calorimeter (DSC), Model Q20, TA Instruments, USA. The DSC experiments were carried out in an ultra-high purity nitrogen atmosphere at a flow rate of 50 mL/min and a heating rate of 10 °C/min. The mechanical properties, tensile strength (TS), elastic modulus − initial slope of stress-strain curve − (E-mod) of the cured propellant samples and the percentage elongation were determined on a Hounsfield universal testing machine (UTM) using dumbbells conforming to ASTM-D-638 type IV at a cross head speed of 50 mm/min at ambient temperature. The calorimetric value (cal-val) [25] and density of the cured propellant formulations were determined with a Parr isoperibol bomb oxygen calorimeter 6200 (under inert nitrogen atmosphere) and a helium gas pycnometer, respectively.

The burning rate of the cured propellant samples was determined by the acoustic emission technique in an inert environment (N_2) at 5.88 MPa, 6.86 MPa, and 7.84 MPa using a 750 cm^3 stainless steel Crawford bomb at 27 °C. The bomb was equipped with a piezoelectric transducer made of Lithium Niobate crystal on a ceramic sole. An acoustic signal was generated by the rapid release of energy accompanying the propellant combustion. The propellant samples were cut in the form of solid strand burning rate (SSBR) samples having dimensions of 150 mm × 6 mm × 6 mm and ignited from one end using Nichrome wire. When

the propellant strand burned, an acoustic pulse was generated and was measured using an oscilloscope. The burning rate of the propellant strand was calculated by dividing the length of the strand by the duration of acoustic pulse. The error in the measured burning rate, in the range of ± 2%, may be due to dimensional variation of the propellant strand and length measurement.

2.3 Incorporation of nano- and micron-sized MnO_2 in the composite propellant formulation

Initially, the prepolymer resin (504 g), *i.e.* HTPB, dioctyl adipate (DOA; 150 g) as a plasticizer, along with an antioxidant (5 g), *i.e.* N-phenyl-2-naphthylamine (NONOX-D) and a bonding agent (6 g; a mixture of 1,1,1-trimethylol propane and 1,4-butanediol) were charged to a vertical planetary mixer (volume 15 L) and the whole mixture was mixed well for 30 min, followed by mixing under vacuum for a further 30 min to drive out entrapped air. After this, nano-MnO_2 or micron-MnO_2 (25 g) was added and mixed thoroughly for 10 min before Al powder (~15 μm; 900 g) was added to the mix. After complete addition of the Al, the mixture was mixed for a further 20 min. Subsequently, AP (3375 g; bimodal having particle sizes of 300 μm and 50 μm) was added and mixed in such a way that homogeneity was obtained. The overall mixing temperature was maintained at 40 ± 2 °C. After complete addition of the solid ingredients, the mixing of the composition was continued under vacuum for 30 min. At this stage, toluene diisocyanate (TDI; 35.0 g) was added and mixed for a further 40 min. The composition was then cast into 100 mm inner diameter (ID) moulds by the vacuum casting technique and cured at 50 °C for 5 days [26].

The percentage of nano-MnO_2/micron-MnO_2 used for this study was varied from 0.25 wt.% to 1.0 wt.%.

3 Results and Discussion

Initially, both nano- and micron-sized MnO_2 were fully characterized and their catalytic effect on AP was followed by evaluation in composite propellant formulations.

3.1 Powder X-ray diffraction

The nano-MnO_2/micron-MnO_2 was characterized for its material identification, as well as phase identification, using the powder XRD technique at a scanning rate of 2°/min in a continuous scanning mode and the XRD patterns obtained are presented in Figures 1 and 2. It is clear from the XRD patterns that nano-

MnO_2/micron-MnO_2 are of crystalline nature. The XRD pattern has six clearly distinguishable peaks which correspond to 2θ values of 28.75, 37.44, 41.24, 42.31, 46.06, 56.83, and 60.01, respectively. These peaks are due to nano-MnO_2/micron-MnO_2 phases and are in agreement with the standard data file (JCPDS Card NO 24-0735) [27]. Figures 1 and 2 also clearly reveal broadened peaks at the bases in the case of nano-MnO_2, and confirm its smaller crystallite size compared to micron-MnO_2.

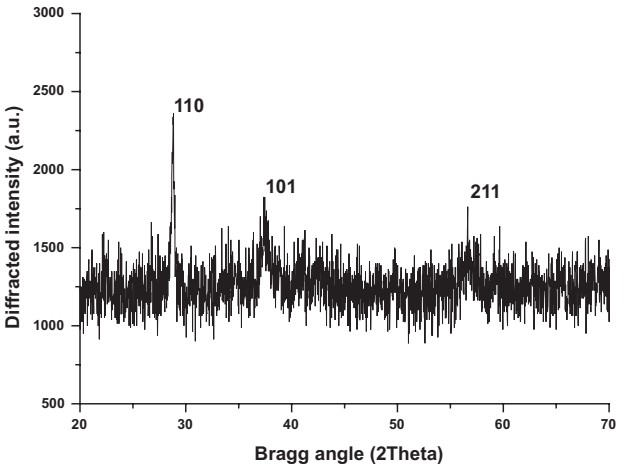

Figure 1. X-ray diffraction pattern of nano-MnO_2

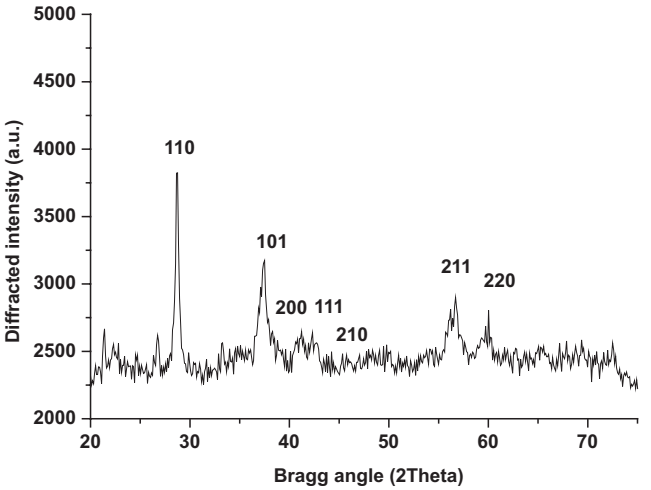

Figure 2. X-ray diffraction pattern of micron-sized MnO_2

3.2 Determination of purity

The purity of nano-MnO_2/micron-MnO_2 was determined by Inductively Coupled Plasma-Atomic Emission Spectroscopy (ICP-AES) using a high temperature argon plasma. The percentage of manganese content in nano- and micron-MnO_2 was found to be 62.97 wt.% and 63.03 wt.% respectively (63.19 wt.% theoretical). Based on the manganese content, the purity of nano-MnO_2/micron-MnO_2 was found to be greater than 99.5 wt.%.

3.3 Determination of particle size by NANOPHOX

The particle size of nano-MnO_2 was determined by NANOPHOX particle size analyser. The results revealed that the surface mean diameter of the product was 51 nm whereas the distribution of the nano particles varied from 36 nm to 75 nm. The particle size of micron-MnO_2 was determined by CILAS and found to be 1.32 μm.

3.4 Determination of particle size and surface morphology

The particle size and surface morphology of nano- and micron-manganese dioxide was also determined by FESEM. The images infer that particles of nano-MnO_2 seemed to very close to spherical in nature and the average particle size was in the region of 45 nm. The surface morphology of micron-sized manganese dioxide appeared to be irregular in shape with an average particle size in the region of 1.31 μm. The FESEM of micron-sized manganese dioxide is shown in Figure 3.

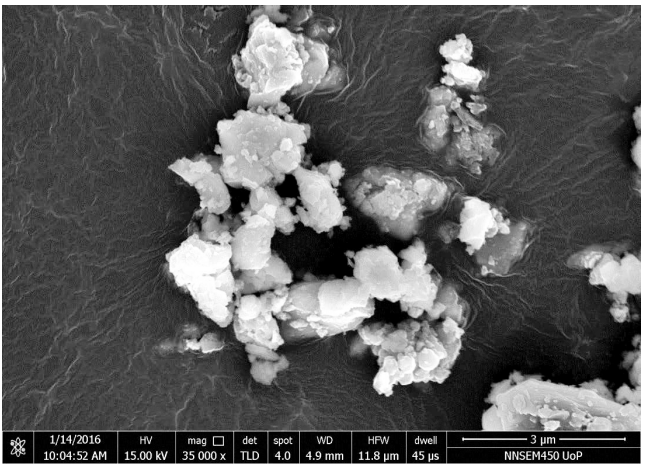

Figure 3. Field emission − scanning electron microscopic image of micron-sized MnO_2

3.5 Determination of the specific surface area by BET surface area analyser

The specific surface area of nano-MnO_2 and micron-MnO_2 was determined by using a BET specific surface area analyser at liquid nitrogen temperature. The results revealed that the specific surface area of nano-MnO_2 was 24.22 m^2/g, whereas that of micron-MnO_2 was 4.4 m^2/g. It is clear from above data that the nano-MnO_2 is finer than the micron-MnO_2, therefore a better catalytic effect was envisaged.

3.6 Catalytic effect of nano- and micron-sized MnO_2 on ammonium perchlorate

The DSC samples were prepared by blending AP and MnO_2 in a mortar using a pestle. The DSC thermograms obtained for nano-MnO_2 and micron-MnO_2 are shown in Figures 4 and 5, respectively. The thermograms clearly indicated that on addition of nano-MnO_2/micron-MnO_2, the decomposition temperature of AP was decreased. It is clear from Figure 4 that the decomposition temperature of AP without any ballistic modifier was 463.25 °C, whereas on addition of nano-MnO_2 at 0.367 wt.%, 0.735 wt.%, 1.101 wt.% and 1.468 wt.% (corresponding to 0.25 wt.%, 0.5 wt.%, 0.75 wt.% and 1.0 wt.% in the propellant composition) the decomposition temperature became 373.03 °C, 358.59 °C, 349.89 °C and 346.14 °C, respectively. This effect was found to be less marked in the case of micron-MnO_2, as shown in Figure 5, where the decomposition temperature of AP with 0.367 wt.%, 0.735 wt.%, 1.101 wt.% and 1.468 wt.% became 393.88 °C, 377.90 °C, 371.71 °C and 364.80 °C, respectively. This finding infers further that nano-MnO_2 has a very good catalytic effect on the thermal decomposition of AP due to its higher specific surface area in comparison to that of micron-MnO_2.

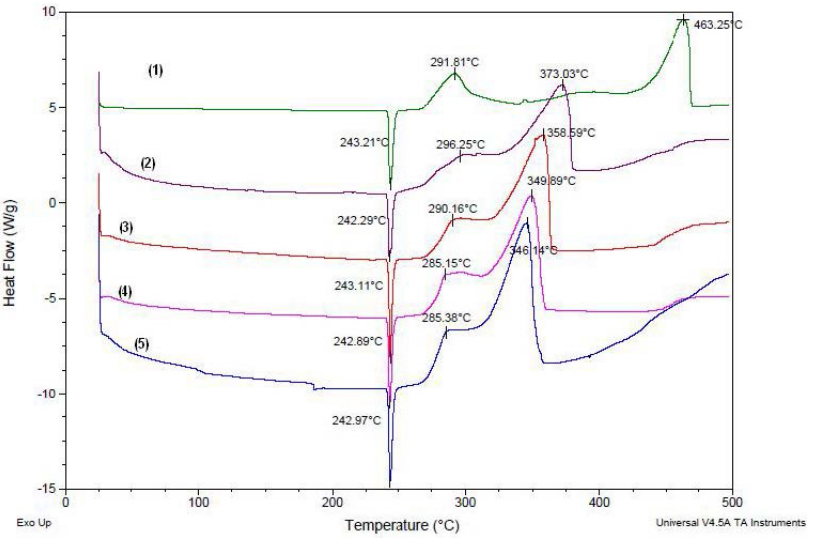

Figure 4. DSC thermograms of AP (1) and with nano-MnO_2 content: 0.367 wt.% (2), 0.735 wt.% (3), 1.101 wt.% (4), 1.468 wt.% (5)

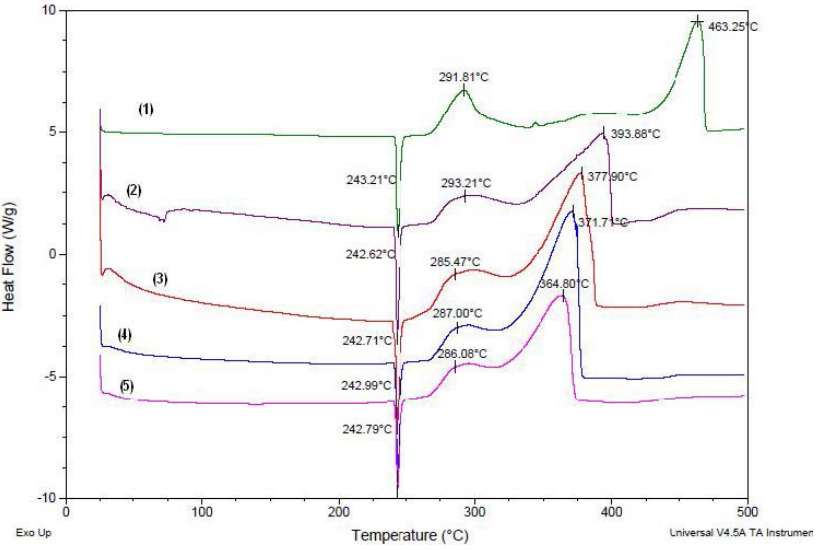

Figure 5. DSC thermograms of AP (1) and with micron-sized MnO_2 content: 0.367 wt.% (2), 0.735 wt.% (3), 1.101 wt.% (4), 1.468 wt.% (5)

3.7 Evaluation of nano- and micron-sized MnO_2 in composite propellant formulations

The propellant formulations were processed by incorporation of nano-MnO_2/micron-MnO_2, from 0.25 wt.% to 1.0 wt.%, by replacing coarse AP and the effects on viscosity built-up, and the thermal, mechanical and ballistic properties were studied. The formulation details are given in Table 1.

Table 1. Formulation details of the propellant compositions studied

Sr. No.	Ingredients	Compositions [wt.%]				
		Reference	Comp. 1	Comp. 2	Comp. 3	Comp. 4
1	Binder (HTPB+TDI+DOA)	14.00	14.00	14.00	14.00	14.00
2	AP Coarse (300 μm)	52.50	52.25	52.00	51.75	51.50
3	AP Fine (50 μm)	15.50	15.50	15.50	15.50	15.50
4	Aluminium powder (15 μm)	18.00	18.00	18.00	18.00	18.00
5	Nano-MnO_2/micron-MnO_2	-	0.25	0.50	0.75	1.00

3.7.1 Effect of nano- and micron-sized MnO_2 on viscosity

Table 2. Data on the effect of nano- and micron-sized MnO_2 on the viscosity, and the mechanical properties and density of the composite propellant formulations

Sr. No.	HTPB/AP/Al (14/68/18 wt.%) with		Viscosity at 40 °C [Pa·s]	Tensile strength [MPa]	E-modulus [MPa]	Elongation [%]	Density [kg/m^3]
	nano-MnO_2 [wt.%]	micron-MnO_2 [wt.%]					
1	-	-	670	0.62	3.43	45.00	1777
2	0.25	-	730	0.71	3.70	41.10	1777
3	0.50	-	774	0.75	4.04	37.33	1779
4	0.75	-	832	0.76	4.36	33.62	1780
5	1.00	-	865	0.80	4.63	31.62	1781
6	-	0.25	704	0.68	3.64	42.22	1777
7	-	0.50	756	0.73	4.02	39.47	1779
8	-	0.75	795	0.74	4.12	37.38	1781
9	-	1.00	843	0.76	4.25	35.22	1783

The end of mix (EOM) viscosity data of the studied compositions are listed in Table 2. The data clearly indicate that as the nano-MnO_2 content in the

composition was increased, the end of mix (EOM) viscosity of the propellant slurry also increased, *i.e.*, from 730 Pa·s to 865 Pa·s, in comparison to the viscosity of the reference composition (670 Pa·s). The increase in viscosity may be due to the finer particle size and the higher specific surface area of nano-MnO_2 in comparison to micron-MnO_2.

3.7.2 Effect of nano- and micron-sized MnO_2 on the mechanical properties

The data on the mechanical properties are presented in Table 2. It is clear from these data that as the percentage of nano-MnO_2 in the composition was increased, the tensile strength and E-modulus increased marginally, while the percentage elongation decreased. This may be attributed to the increase in packing density of the propellant composition on addition of nano-MnO_2. Thus, the values of TS and E-modulus for nano-MnO_2 was increased from 0.71 MPa and 3.70 MPa to 0.80 MPa and 4.63 MPa, respectively, in comparison to 0.62 MPa and 3.43 MPa for the reference composition. However, a decreasing trend in % elongation was observed for the studied compositions compared to the reference composition.

3.7.3 Effect of nano- and micron-sized MnO_2 on the density

The data on the densities of the cured propellant formulations are given in Table 2. It is clear from these data that the density of the nano-MnO_2 and micron-MnO_2 based formulations had almost same density as the reference composition (1777 kg/m^3). However, there was a marginal improvement in the density when the concentration used was above 0.5 wt.%, due to higher density of MnO_2 compared to AP.

3.7.4 Effect of nano- and micron-sized MnO_2 on the thermal properties

The thermal properties of the studied compositions containing nano- and micron-sized MnO_2, together with the reference composition, were evaluated and the data on the endotherms/exotherms are listed in Table 3. The reference composition showed an endotherm at 247 °C due to the phase change of AP from orthorhombic to cubic. After that, a small decomposition peak was observed around 304 °C, followed by a sharp decomposition peak at 403 °C. On incorporation of nano-MnO_2, the final decomposition peak was shifted from 397 °C to 385 °C as the concentration of MnO_2 was increased from 0.25 wt.% to 1.0 wt.%. These results revealed that nano-MnO_2 is very effective in catalysing the decomposition of the composite propellant formulations. The same trend has also been observed with micron-MnO_2, but to a lesser extent, in comparison to nano-MnO_2.

Table 3. Data on the effect of nano- and micron-sized MnO_2 on the thermal decomposition temperature of the composite propellant formulations

Sr. No.	HTPB/AP/Al (14/68/18 wt.%) with		Endotherm [°C]	Exotherm [°C]
	nano-MnO_2 [wt.%]	micron-MnO_2 [wt.%]		
1	-	-	247	403
2	0.25	-	247	397
3	0.50	-	246	387
4	0.75	-	246	387
5	1.00	-	247	385
6	-	0.25	248	402
7	-	0.50	247	401
8	-	0.75	247	394
9	-	1.00	248	392

3.8 Effect of nano- and micron-sized MnO_2 on the ballistic properties

3.8.1 Effect of nano- and micron-sized MnO_2 on the calorimetric value

Table 4. Data on the ballistic properties of the studied compositions using nano- and micron-sized MnO_2

Sr. No.	Composition		Solid strand burning rate (SSBR) at MPa [mm/s]			Pressure Exponent, n-value	cal-val [Cal/g]
			5.88	6.86	7.88		
1	Reference composition: HTPB/AP/Al (14/68/18 wt.%)		6.00	6.11	6.55	0.35	1550
2	with nano-MnO_2 [wt.%]	0.25	6.82	7.18	7.64	0.37	1543
3		0.50	6.89	7.36	7.76	0.39	1540
4		0.75	6.96	7.43	7.95	0.41	1533
5		1.00	7.10	7.54	8.02	0.42	1525
6	with micron-MnO_2 [wt.%]	0.25	6.65	7.03	7.43	0.36	1541
7		0.50	6.77	7.12	7.61	0.38	1537
8		0.75	6.85	7.32	7.91	0.40	1531
9		1.00	6.97	7.41	7.85	0.41	1523

The calorimetric values (cal-val) of the studied propellant formulations are listed in Table 4. It is clear from these data that the cal-val of the reference composition was 1550 cal/g, whereas on incorporation of nano-MnO_2 and micron-MnO_2 it

decreased slightly. The decrease in cal-val is attributed to the inertness of nano-MnO_2 and micron-MnO_2 in place of AP.

3.8.2 Effect of nano- and micron-sized MnO_2 on the burning rate

The burning rates were determined by the acoustic emission technique in an inert atmosphere at 6.86 MPa [25], and the data obtained are listed in Table 4. It is clear from these data that as the percentage of nano-MnO_2 was increased, the burning rate also increased accordingly. The table also shows that a 2% increase in burning rate was observed with nano-MnO_2 in comparison to micron-MnO_2 at 1.0 wt.%, however, in comparison to the reference composition, there was 23% enhancement in the burning rate. The burning rate enhancement using nano- and micron-MnO_2 in the compositions clearly infers that as the concentration of the catalyst reaches the level of 1.0%, the burning rate enhancement becomes saturated, which indicated that this is the optimum concentration, and consequently compositions with >1 wt.% concentration were not studied. The increase in burning rate may be due to the higher specific surface area of nano-MnO_2 in comparison to that of micron-MnO_2.

3.8.3 Effect of nano- and micron-sized MnO_2 on the pressure exponent (n)

The pressure exponent (n) was determined using SSBR data at different pressures, by plotting a curve of $\log_e$ (burning rate) *vs.* $\log_e$ (pressure) and calculating the pressure exponent from the slope of the curve [29]. The data obtained are listed in Table 4. The pressure exponent of the reference composition was 0.35, and on addition of nano-MnO_2 and micron-MnO_2 the pressure exponent value increased from 0.37 to 0.42 and 0.36 to 0.41, respectively, as the catalyst concentration was increased from 0.25 wt.% to 1.0 wt.%.

4 Conclusions

A successful attempt has been made to incorporate nano-MnO_2 in composite propellant formulations, from 0.25 wt.% to 1 wt.% by replacing coarse AP, having 86 wt.% solid loading, and its effects on the end of mix viscosity, and the mechanical, thermal and ballistic properties were studied. The data revealed that there was an increase in end of mix viscosity from 730 Pa·s to 865 Pa·s on incorporation of nano-MnO_2 from 0.25 wt.% to 1.0 wt.%, whereas the EOM viscosity of the reference composition was 670 Pa·s at the same temperature, while no changes in the mechanical properties were observed. Furthermore, nano-MnO_2 was found to be effective in lowering the thermal decomposition

temperature to 346.94 °C, in comparison to micron-sized MnO_2 (364.8 °C), at 1 wt.%. The data on the burning rate revealed that there is a 2% enhancement in the burning rate with nano-MnO_2 in comparison to micron-sized MnO_2, at 1.0 wt.% concentration. However, in comparison to the reference composition, 23% enhancement in the burning rate was observed. Furthermore, approximately the same pressure exponent value was observed on addition of nano-MnO_2 and micron-sized MnO_2 in the studied composite propellant formulations. The developed compositions may find application where moderately high burning rate propellants are required.

Acknowledgments
Authors would like to thank Mr K. I. Dhabbe and Mrs Lalita Jawale for the laboratory facilities and ballistic evaluation.

References

[1] Dey, A.; Sikder, A. K.; Talwar, M. B.; Chattopadhyay, S. Towards New Directions in Oxidizers-Energetic Fillers for Composite Propellants: An Overview. *Cent. Eur. J. Energ. Mater.* **2015**, *12*(2): 377-399.
[2] Jain, S.; Mehilal; Singh, P. P.; Bhattacharya, B. Evaluation of Potassium Perchlorate as Burning Rate Modifier in Composite Propellant Formulations. *Cent. Eur. J. Energ. Mater.* **2016**, *13*(1): 231-245.
[3] Oberth, A. E.; Bruenner, R. S. Polyurethane-based Propellant. In: *Propellant, Manufacturing Hazard and Testing* (Boyers, C.; Klager, K., Eds.), American Chemical Society, Washington D.C. **1969**, pp. 84-121; ISBN 9780841200890.
[4] Yaman, H.; Celik, V.; Degrimenci, E. Experimental Investigation of Factors Affecting the Burning Rate of Solid Rocket Propellant. *Fuel* **2014**, *115*: 794-803.
[5] Boldyrev, V. V. Thermal Decomposition of Ammonium Perchlorate. *Thermochim. Acta* **2006**, *443*: 1-36.
[6] Kohga, M. Burning Characteristic and Thermo Chemical Behaviour of AP/HTPB Composite Propellant Using Coarse and Fine AP Particle. *Propellants Explos. Pyrotech*. **2011**, *36*: 57.
[7] Kishore, K.; Prasad, G. A Review on Decomposition/Deflagration of Oxidizer and Binder in Composite Solid Propellant. *Def. Sci. J.* **1979**, *20*: 39-54.
[8] Jacobs, P. M. V.; Whithead, H. M. Decomposition and Combustion of Ammonium Perchlorate. *Chem. Rev*. **1969**, *4*: 551-590.
[9] Kishore, K.; Verneker, V. R. P.; Sunitha, M. R. Effect of Catalyst Concentration on Burning Rate of Composite Solid Propellants. *AIAA J*. **1977**, *15*: 1649-1651.
[10] Kishore, K.; Sunitha, M. R. Mechanism of Catalytic Activity of Transition Metal Oxide on Solid Propellant Burning Rate. *Combust. Flame* **1978**, *33*: 311-314.

[11] Gore, G. M.; Tipare, K. R.; Bhatewara, R. G.; Prasad, U. S.; Gupta, M.; Mane, S. R. Evaluation of Ferrocene Derivatives as Burn Rate Modifiers in AP/HTPB-based Composite Propellants. *Def. Sci. J.* **1999**, *49*(2): 151-158.
[12] Ghosh, K.; Behera, S.; Kumar, A.; Padale, B. G.; Deshpande, D. G.; Kumar, A.; Gupta, M. Studies on Aluminized, High Burning Rate, Butacene® Based, Composite Propellants. *Cent. Eur. J. Energ. Mater.* **2014**, *11*(3): 323-333.
[13] Pang, W.; DeLuca, T. L.; Fan, X.; Maggi, F.; Xu, H.; Xie, W.; Shi, X. Effects of Different Nano-sized Metal Oxide Catalysts on the Properties of Composite Solid Propellants. *Combust. Sci. Technol.* **2016**, *188*(3): 315-328.
[14] Kshirsagar, D. R.; Jain, S.; Jawalkar, S. N.; Naik, N. H.; Pawar, S.; Maurya, M. Evaluation of Nano-Co_3O_4 in HTPB-based Composite Propellant Formulations. *Propellants Explos. Pyrotech.* **2016**, *41*(2): 304-311.
[15] Kshirsagar, D.; Kurva, R.; Dhabbe, K.; Jawale, L.; Sudhir Khire, V.; Mehilal Effect of Nano Cr_2O_3 in HTPB/AP/Al Based Composite Propellant Formulations. *Def. Sci. J.* **2016**, *66*(2): 100-106.
[16] Chen, S.; Zhu, J.; Huang, H.; Zeng, G.; Nie, F.; Wang, X. Facile Solvothermal Synthesis of Graphene-MnOOH Nanocomposites. *J. Solid State Chem.* **2010**, *183*(11): 2552-2557.
[17] Li, N.; Geng, Z.; Cao, M.; Ren, L.; Zhao, X.; Liu, B.; Tian, Y.; Hu, C. Well-dispersed Ultrafine Mn_3O_4 Nanoparticles on Graphene as a Promising Catalyst for the Thermal Decomposition of Ammonium Perchlorate. *Carbon* **2013**, *54*: 124-132.
[18] Han, A., Liao, J., Ye, M., Li, Y., Peng, X. Preparation of Nano-$MnFe_2O_4$ and Its Catalytic Performance of Thermal Decomposition of Ammonium Perchlorate. *Chinese Journal of Chemical Engineering* **2011**, *19*(6): 1047-1051.
[19] Chandru, R. A.; Patra, S.; Oommen, C.; Munichandraiah, N.; Raghunandan, B. N. Exceptional Activity of Mesoporous β-MnO_2 in the Catalytic Thermal Sensitization of Ammonium Perchlorate. *J. Mater. Chem.* **2012**, *22*(14): 6536-6538.
[20] Naya, T.; Kohga, M. Burning Characteristics of Ammonium Nitrate-based Composite Propellants Supplemented with MnO_2. *Propellants Explos. Pyrotech.* **2013**, *38*(1): 87-94.
[21] Kohga, M.; Naya, T. Thermal Decomposition Behaviors and Burning Characteristics of AN/RDX-based Composite Propellants Supplemented with MnO_2 and Fe_2O_3. *J. Energ. Mater.* **2015**, *33*(4): 288-304.
[22] Kawamura, K. Influence of Copper Oxide Catalysts on the Burning Rate of a Composite Propellant. *Kogyo Kayaku* **1989**, *50*(5): 415-424.
[23] Kishore, K.; Verneker, V. R. P.; Sunitha, M. R. Action of Transition Metal Oxides on Composite Solid Propellants. *AIAA J.* **1980**, *18*(11): 1404-1405.
[24] Singh, G.; Kapoor, I. P. S.; Dubey, S.; Siril, P. F. Preparation, Characterization and Catalytic Activity of Transition Metal Oxide Nanocrystals, *Journal of Scientific Conference Proceeding*, **2009**, *1*: 11-17.
[25] Jawale, L. S.; Dey, C.; Mehilal; Gupta, M.; Bhattacharya, B. Effect of Experiment Environment on Calorimetric Value of Composite Solid Propellants. *Def. Sci. J.* **2013**, *63*(5): 467-472

[26] Kshirsagar, D. R.; Sudhir; Mehilal; Singh, P. P.; Bhattacharya, B. Evaluation of Nano-Fe_3O_4 in Composite Propellant Formulation. *Int. J. Energ. Mater. Chem. Propul*. **2013**, *12*(6): 463-474.
[27] Zheng, D.; Sun, S.; Fan, W.; Yu, H.; Fan, C.; Cao, G.; Yin, Z.; Song, X. One Step Preparation of Single Crystalline β-MnO_2 Nanotubes. *J. Phys. Chem., B* **2005**, *109*: 16439-16443.
[28] Gupta, G.; Jawale, L.; Mehilal; Bhattacharya, B. Various Methods for the Determination of the Burning Rates of Solid Propellants – an Overview. *Cent. Eur. J. Energ. Mater.* **2015**, *12*(3): 593-620.
[29] Mehilal; Jawalkar, S. N.; Kurva, R.; Nandagopal, S.; Dombe, G.; Singh, P. P.; Bhattacharya, B. Studies on High Burning Rate Composite Propellant Formulations Using TATB as Pressure Index Suppressant. *Cent. Eur. J. Energ. Mater.* **2012**, *9*: 237-249.